



Integrated Arctic Observation System

Research and Innovation Action under EC Horizon2020
Grant Agreement no. 727890

Project coordinator:
Nansen Environmental and Remote Sensing Center, Norway


Deliverable 6.22

Sea ice products from satellite scatterometers and passive microwave sensors

Start date of project:	01 December 2016	Duration:	63 months
Due date of deliverable:	31 October 2021	Actual submission date:	15 November 2021
Lead beneficiary for preparing the deliverable:	IFREMER		
Person-months used to produce deliverable:	6		

Authors: Fanny Girard-Ardhuin, Jean-François Pollé

Version	DATE	CHANGE RECORDS	LEAD AUTHOR
1.0	25/10/2021	V1	F. Girard-Ardhuin
1.1	27/10/2021	V2 Review	G. Heygster
1.2	28/10/2021	V3 Corrections incorporated	F. Girard-Ardhuin
1.3	05/11/2021	Technical Review and formatting	K. Lygre
1.4	15/11/2021	Final review and submission	Stein Sandven/Hanne Sagen

Approval X	Date: 15 November 2021	Sign.  Coordinator
----------------------	---------------------------	--

USED PERSON-MONTHS FOR THIS DELIVERABLE					
No	Beneficiary	PM	No	Beneficiary	PM
1	NERSC		24	TDUE	
2	UiB		25	GINR	
3	IMR		26	UNEXE	
4	MISU		27	NIVA	
5	AWI		28	CNRS	
6	IOPAN		29	U Helsinki	
7	DTU		30	GFZ	
8	AU		31	ARMINE	
9	GEUS		32	IGPAN	
10	FMI		33	U SLASKI	
11	UNIS		34	BSC	
12	NORDECO		35	DNV GL	
13	SMHI		36	RIHMI-WDC	
14	USFD		37	NIERSC	
15	NUIM		38	WHOI	
16	IFREMER	6	39	SIO	
17	MPG		40	UAF	
18	EUROGOOS		41	U Laval	
19	EUROCEAN		42	ONC	
20	UPM		43	NMEFC	
21	UB		44	RADI	
22	UHAM		45	KOPRI	
23	NORUT		46	NIPR	
			47	PRIC	

DISSEMINATION LEVEL		
PU	Public, fully open	X
CO	Confidential, restricted under conditions set out in Model Grant Agreement	
CI	Classified, information as referred to in Commission Decision 2001/844/EC	

EXECUTIVE SUMMARY

This report describes the work done at Ifremer on satellite remote sensing over sea ice using different microwave sensors, in particular work done in WP6 and linked to data delivered through WP2.

We present and assess the data that have been prepared and/or improved (exploited) during the INTAROS project. This refers to data characterization, making the data accessible, creating new datasets, extended the time series from satellites. This also includes data upgraded in the framework of overlapping projects (as for instance CMEMS) but not made available before INTAROS.

This document focus on how existing observations and data products can enhance the existing observation system through data exploitation.

Table of Contents

Table of Contents	3
1. Introduction	4
2. Active and passive microwave data for sea ice applications	4
2.1 Introduction	4
2.2 Low resolution sea ice displacement dataset	4
2.3 Medium resolution sea ice displacement dataset	5
3. New CFOSAT data for sea ice application	6
3.1 Introduction	6
3.2 Backscatter fields	7
Number of data	7
Spatial coverage	8
Example of backscatter field.....	8
Noise level	9
3.3. Sea ice/open water detection	10
3.4 Sea ice drift	10
3.5 Sea ice type.....	12
4. Conclusion and further plans	12
5. Data exploitation	13
6. References	13

1. Introduction

In this report, we show how the Earth Observation satellite data can be used for sea ice application and in particular for the Arctic monitoring. This report is dedicated to scatterometer sensors used in addition to radiometer. Existing long-term satellite products have been updated and are presented in this report. New data by CFOSAT are presented to continue the times series, the data have become available with much delay and are still in calibration/validation activity that is presented here briefly. The perspective is that these new data will be at least as good as the previous ones by ASCAT and QuikSCAT and improved the existing long-term time series by giving the possibility of extending it.

2. Active and passive microwave data for sea ice applications

2.1 Introduction

Scatterometer active data are used originally for ocean wind estimates, but it can also be used for sea ice parameters. Ifremer has a long expertise on the sea ice derived scatterometer parameters since the 1990s. Backscatter data can be used mainly to derive three main sea ice parameters:

- sea ice extent,
- sea ice displacement
- sea ice type

The advantages of using microwave data are twofold: observations can be made during night as well as through cloud cover which is particularly useful for monitoring the polar areas.

In the framework of the INTAROS project, the scatterometer and radiometer have been used to deliver sea ice displacement estimate, the product is presented in a dedicated info-sheet from WP2, "Monitoring of Arctic Sea ice from satellite observations" (Deliverable D2.3). Data is included in the INTAROS data catalogue see <https://catalog-intaros.nersc.no/dataset/sea-ice-displacement-from-satellite-data-at-medium-resolution>

2.2 Low resolution sea ice displacement dataset

Sea ice displacement can be inferred through several technics, Ifremer product has been made using Max Cross Correlation, method and validation are presented in Girard-Ardhuin and Ezraty (2012). Comparisons of the different worldwide existing products have been made, the products are very similar, one comparison study can be found in Sumata et al (2014).

We proposed an enhanced product using both radiometer passive data and scatterometer data, both can be used for sea ice displacement estimate. From the individual estimate of the displacement, we compute a merged product (from both scatterometer and radiometer estimate) which enables higher reliability, more vectors (90% of information from October until April, less in September and May, not in summer) and longer period (September and May) compared to the individual products.

The sea ice displacement vectors are estimated at 3- and 6-day lags, using SSMI radiometer data and QuikSCAT and ASCAT scatterometer data, allowing to have 62.5 km grid resolution Arctic sea-ice maps daily since 1992. By this, Ifremer is able to provide a unique almost 30-year sea ice displacement time series.

This product has been used in many projects and publications for several studies: from pollution detection trajectory to sea ice flux estimate in Fram strait for example.

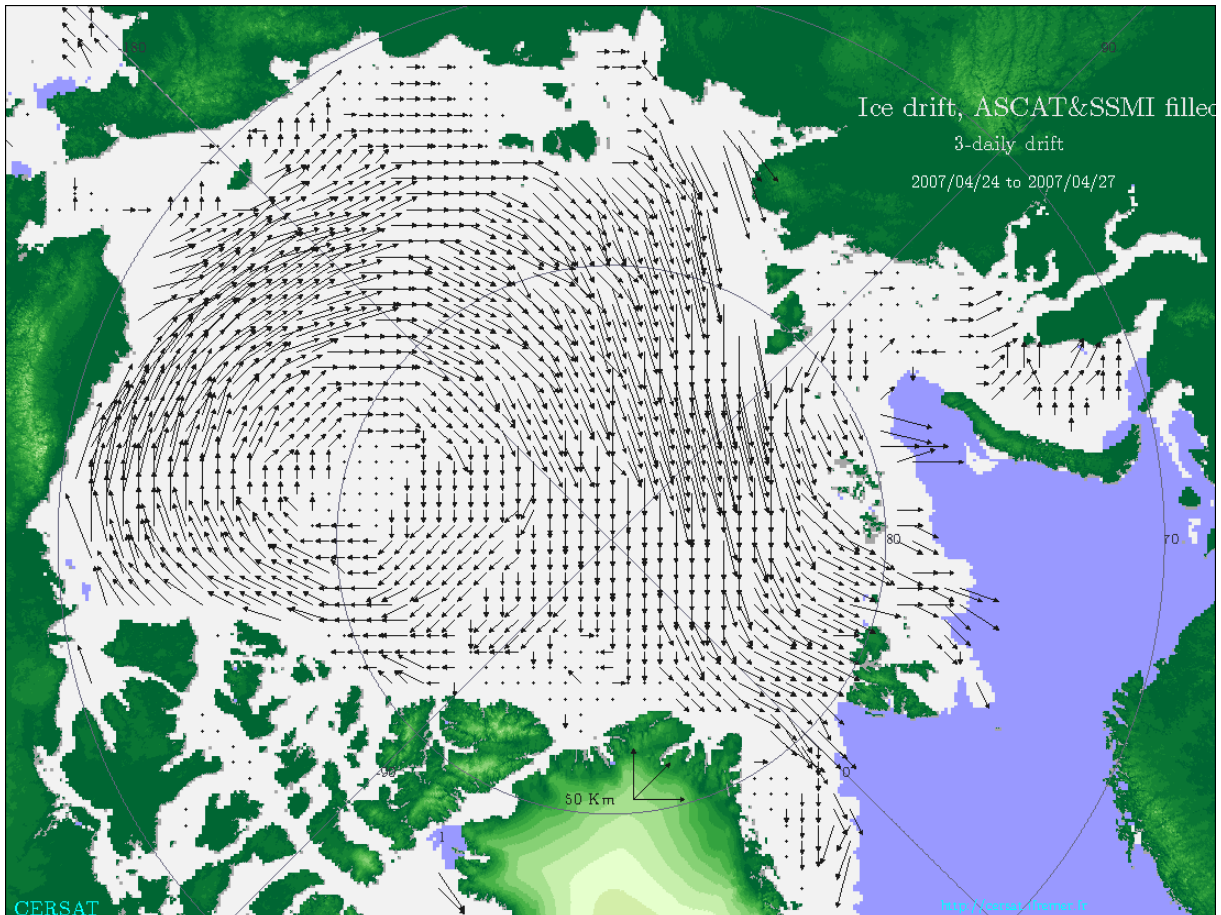


Figure 1 : Arctic mean sea ice displacement at medium resolution at 3 day-lag between April 24 and 27th, 2007 at low resolution using SSMI and ASCAT/MetOp-A sensor data. More than 90% of the vectors are estimated over the sea ice area.

The data are processed routinely, archived, and distributed by the CERSAT at Ifremer, freely, with a userfriendly format and easy access (FTP). A User manual is available on the CERSAT portal and FTP with the data. The dataset is updated with new data and has been provided through WP2 of INTAROS. Figure 1 shows an example of a 3-day sea ice drift map from CERSAT.

2.3 Medium resolution sea ice displacement dataset

Ifremer also provides a medium resolution sea ice displacement dataset derived from the AMSR radiometer:

- AMSR-E between 2002 and 2011,
- AMSR2 between 2012 and present

The sea ice displacement vectors are estimated at 2-, 3- and 6-day lags, the AMSR sensors provide a 31.25 km grid resolution displacement maps daily since 2002 (with a data gap between the two sensors in 2011).

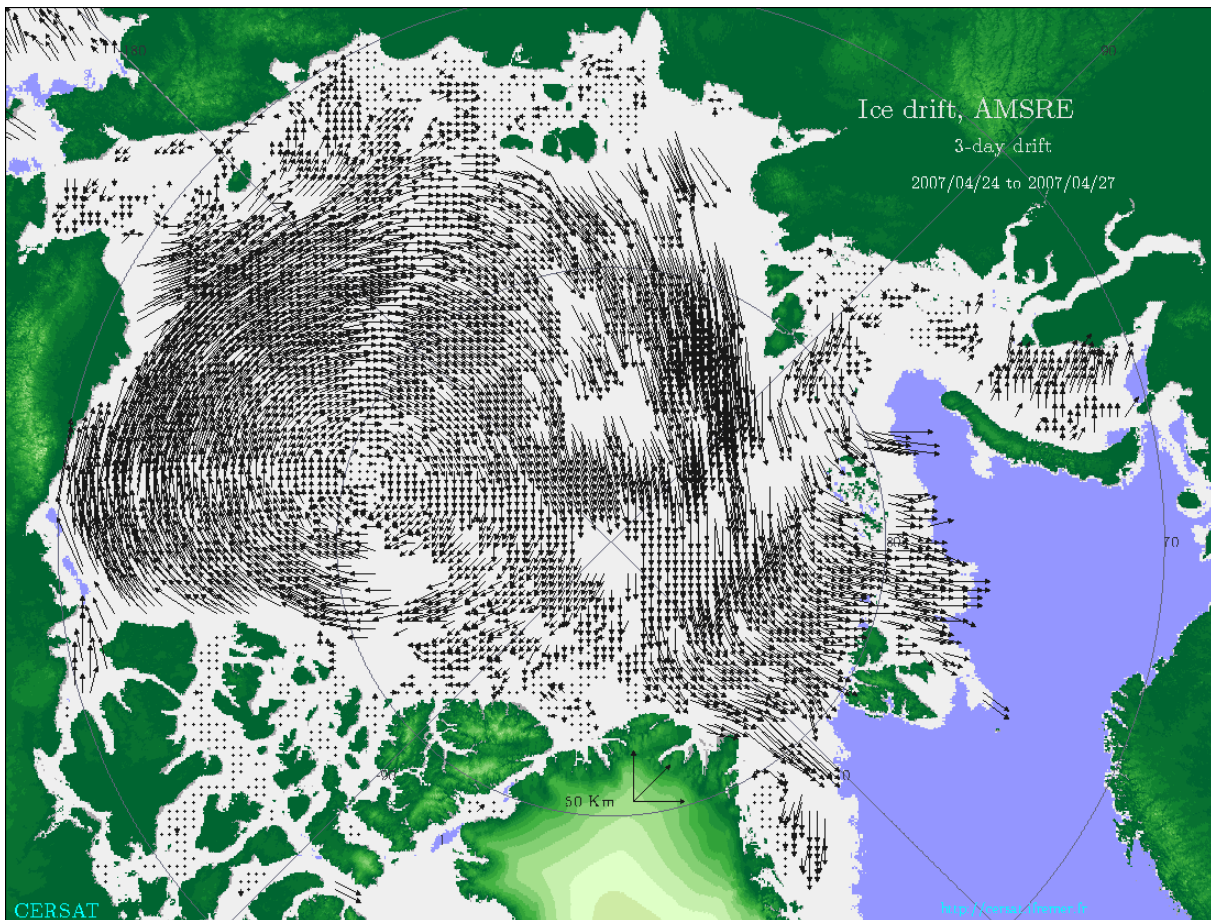


Figure 2: Arctic mean sea ice displacement at medium resolution at 3 day-lag between April 24 and 27th, 2007 at medium resolution using AMSR-E sensor channels data.

The data are processed routinely, archived, and distributed by the CERSAT at Ifremer freely at friendly format and easy access (FTP). User manual is available on the portal and the product is presented in the INTAROS info-sheet.

Figure 2 shows an example of such displacement map. Compared to the example of Figure 1, the angular resolution is better but there are more data gap patches. The use of the low and medium resolution product depends on the application, both are widely used by the scientific community.

3. New CFOSAT data for sea ice application

3.1 Introduction

Two sensors are onboard CFOSAT (Chinese-French Oceanography SATellite):

- SWIM wave sensor
- CSCAT scatterometer.

CFOSAT has been launched in November 2018 and Ifremer is highly involved in the calibration/validation activity that has been started with the SWIM data for wind and wave parameters, that are now provided through the IWWOC center at Ifremer. CSCAT data delivery has been delayed because of different issues and eventually became available to study the polar areas in October 2020 so there was a very short time to study the data for the INTAROS project, this activity continues and will so until the end of the project. These are among the first results one has with the CFOSAT data.

The goal here is

- to show that CFOSAT can be used for sea ice studies,
- to provide qualified CFOSAT sea ice data
- to demonstrate the use of these data jointly to other (buoys, visible data etc.) to observe processes in the MIZ

First results show good results in the Arctic for the beginning of the winter 2020-2021 and the study continues with spring and fall 2021 data presently, the validated sea ice data will be provided to the scientific community through the IWWOC (Ifremer Wind and Wave Operation Center) and CERSAT (all parameters) and INTAROS (for the sea ice displacement parameter).

In this report we study the CSCAT backscatter data that are the basis of the expected sea ice parameters we would like to infer from this sensor.

CSCAT is a Ku-band scatterometer sensor and we use our expertise on the Ku-band QuikSCAT data to study the data over sea ice. Ifremer has a long time series of backscatter data at C and Ku-band from ERS until ASCATs. The CFOSAT data is used to extend this time series which starts in 1991.

Over the 2020-2021 period when CSCAT (Ku-band) are available, we can only use ASCAT data for comparison. The sensors do not have the same frequency (ASCAT is at C-band) but we can use the study we did with both frequencies during the common period we had in 2007-2009 using the ASCAT and the QuikSCAT (Ku-band) data.

3.2 Backscatter fields

Amount of data

Figure 3 shows the amount of data per 12.5 km x 12.5 km pixel resolution on a single day over the Arctic area for ASCAT and CSCAT CFOSAT. We can see that data are distributed as rings and there are a few data gaps for ASCAT. It is well known that the ASCAT geometry has a limited amount of data for one day, but the CFOSAT map shows very high amounts of data with more than 100 and up to 200 in the Central Arctic. This point supports the reliability of the daily maps made from the individual backscatter values.

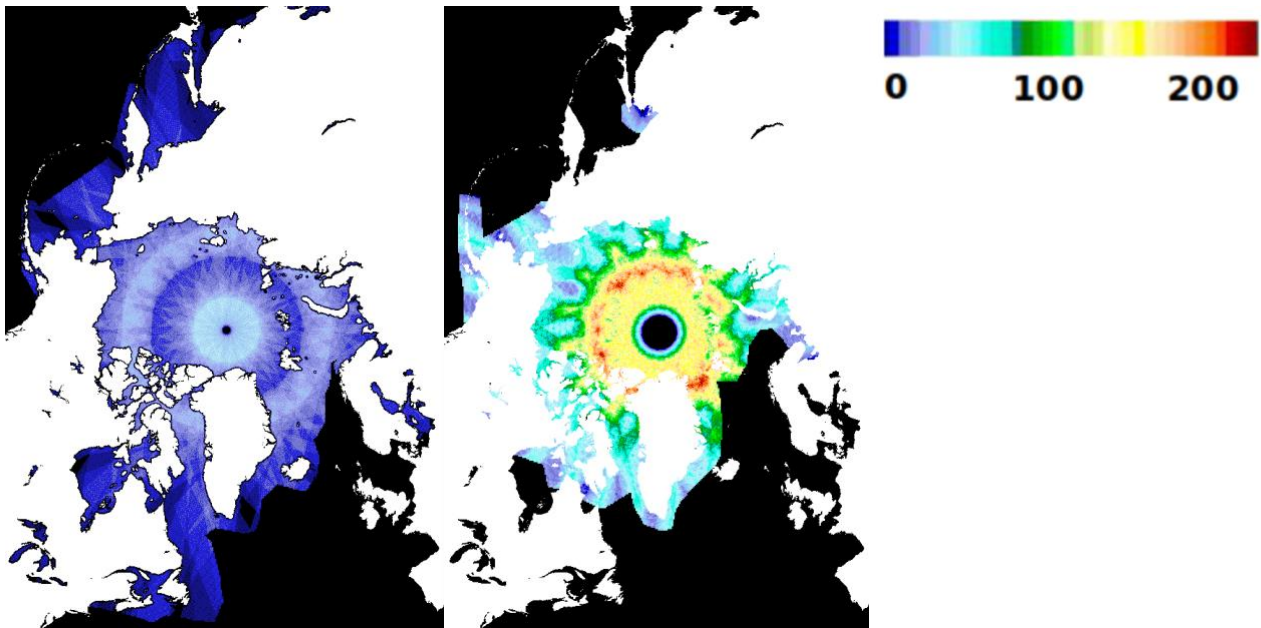


Figure 3: Number of scatterometer data available for one day over the Arctic area. Left: ASCAT, right: CFOSAT.

Spatial coverage

The CSCAT spatial coverage for one day is very good for the Arctic and is of interest for the Antarctic area where sea ice reaches lower latitudes and for example is not fully covered by a single ASCAT sensor. On the contrary, there is a large data gap at the North pole with CSCAT.

Example of backscatter field

Swath data have been used to build an incidence-adjusted map at constant incidence (Gohin and Cavanié, 1992) as it is done for ASCAT and ERS, it is mandatory for a geophysical use over the sea ice area.

Figure 4 shows an example of ASCAT C-band data and CFOSAT Ku-band on the same day during winter. There is the same pattern with high backscatter values (red, yellow, and green) at the North of Canada corresponding to multiyear sea ice and low backscatter value (blue) near the Russian coast for first year sea ice.

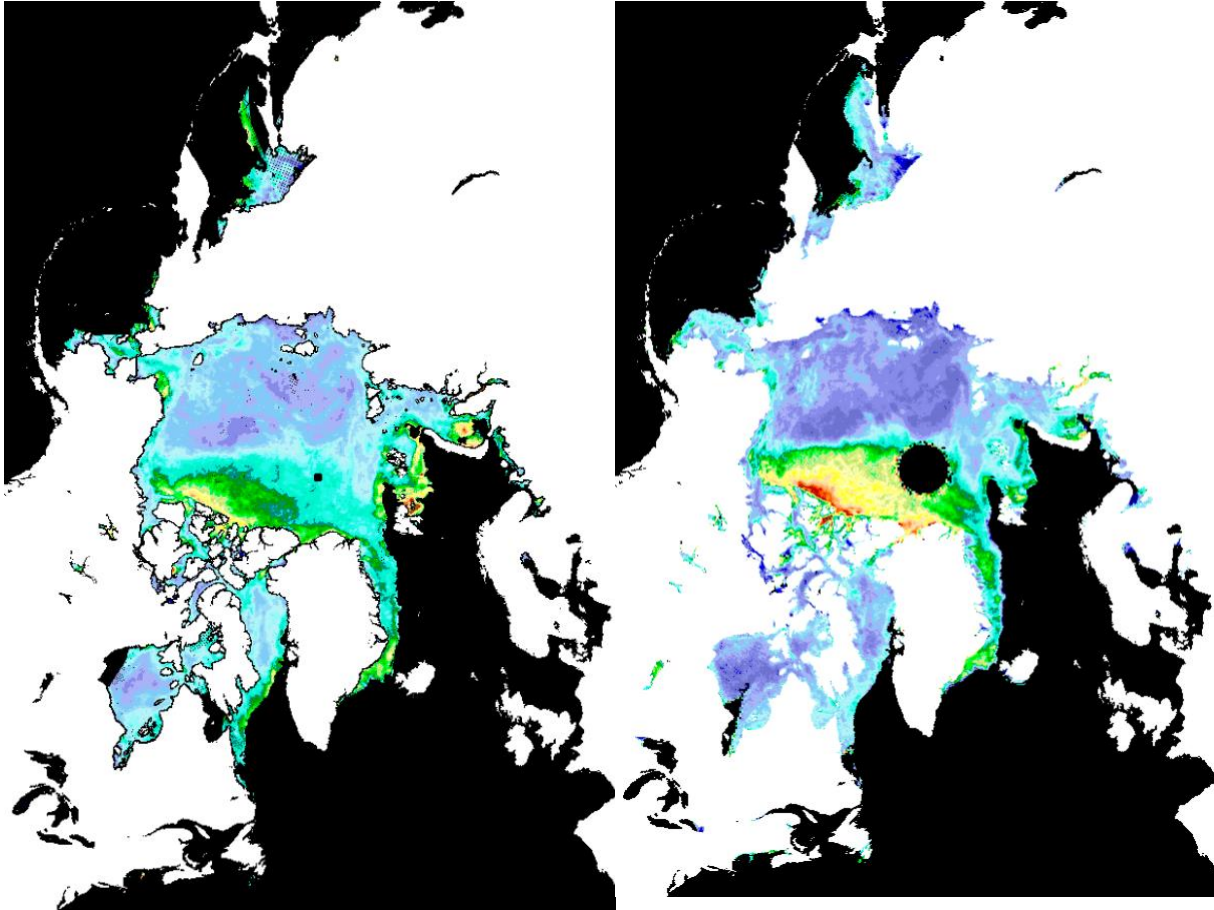


Figure 4: Backscatter map for January 16th, 2021, over the Arctic area. Left: ASCAT, right: CFOSAT. Color bar, see Figure 3. Backscatter values in blue are low, those in green, yellow and red are high.

We study the behavior of the backscatter field evolution from September until the end of winter showing the growing sea ice extent of first year ice with low backscatter values. We can also see that sea ice moves and we compared this with sea ice displacement maps from the ASCAT and SSMI sensors. Values are of course different because of the difference of the frequency, they are not directly to be compared, only qualitatively.

Noise level

The noise level can be estimated from the difference of the backscatter for a day to the next one assuming that the difference is only due to the uncertainty of the determination of the backscatter level (no evolution). We can compare the results to the results we had for ERS, QuikSCAT and ASCAT. Figure 5 shows an example of the results for one day for both sensors ASCAT and CFOSAT.

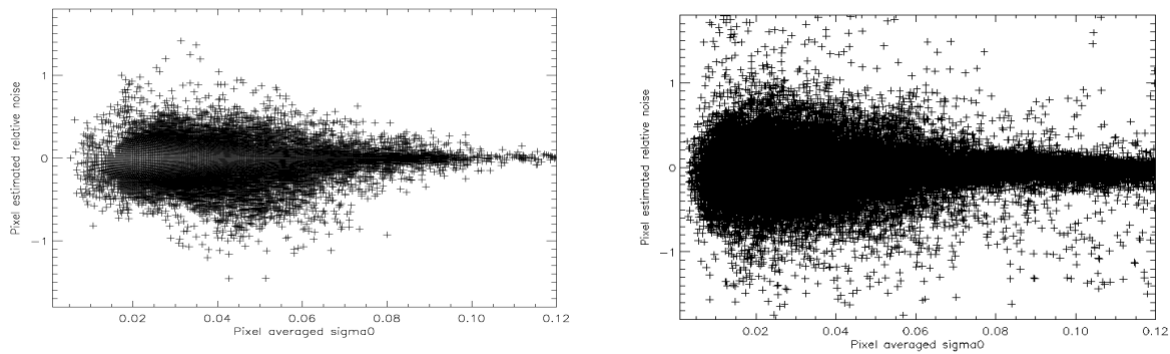


Figure 5: Estimated relative noise level as a function of backscatter values (in linear dB unit) for January 21st, 2021 over the Arctic area. Left ASCAT, right CFOSAT.

Compared to previous studies, the CFOSAT noise level is high: it is centered on zero, it is larger for low backscatter values than for high backscatter values as expected but has many values higher than 1 which was not the case for the other sensors. This should be investigated through the winter season.

3.3. Sea ice/open water detection

The standard deviation of the backscatter can be used to separate sea ice from open water. Figure 6 shows an example using CFOSAT with low standard deviation over the sea ice area and high standard deviation over the open water area. The discrimination is not as reliable as using ASCAT so we may have to use another method. This is ongoing work, and it will be continued during the cold season.

3.4 Sea ice drift

We applied the Ifremer algorithm (Girard-Ardhuin and Ezraty, 2012) over the CFOSAT daily backscatter field to infer sea ice drift maps. Figure 7 shows an example at 3-day lag in January: the pattern of the vectors is like the ASCAT one for the same day. This shows that CFOSAT CSCAT sensor can be used to continue the long-term sea ice displacement time series of CERSAT/Ifremer, these data will be provided through the CERSAT and INTAROS portals, this is also included in the CMEMS multiyear products to be delivered by Ifremer (Le Traon et al. 2021).

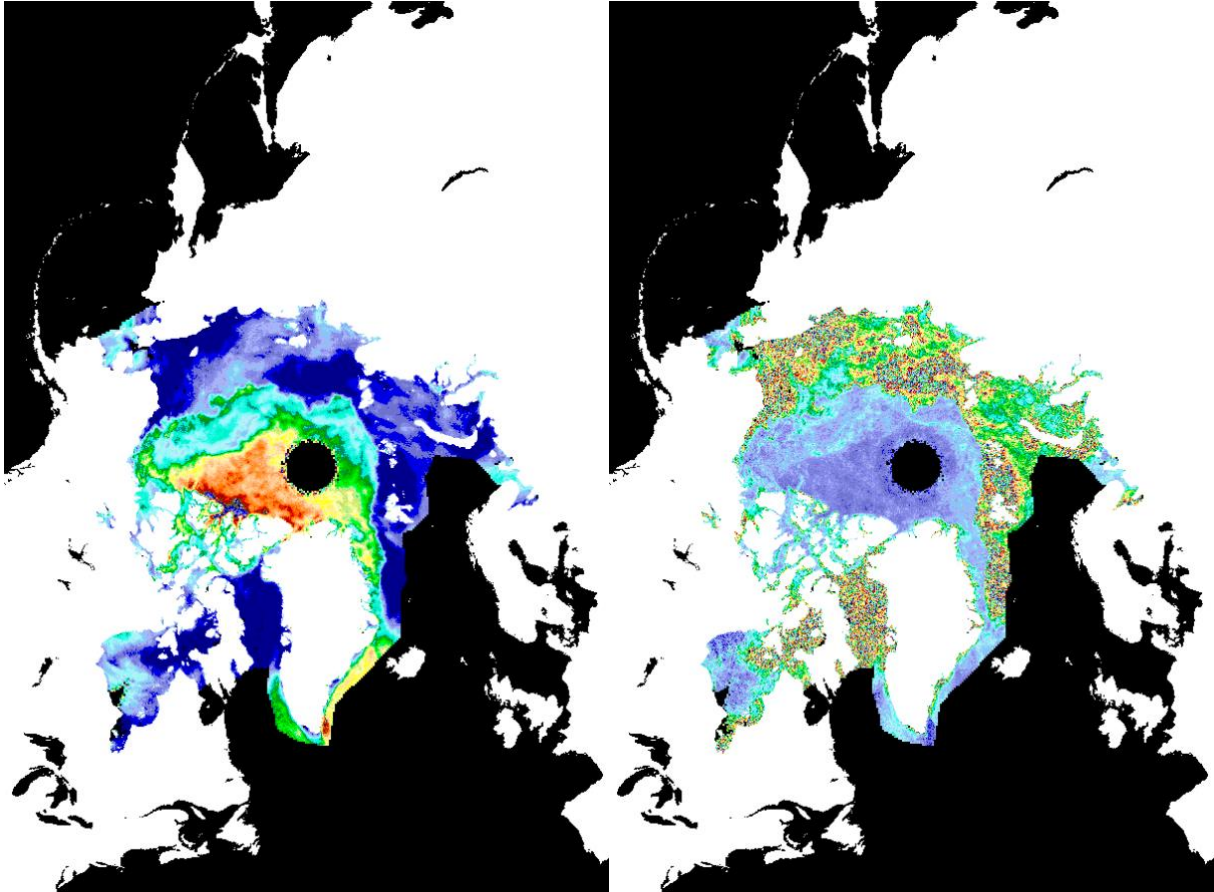


Figure 6: CFOSAT Backscatter (left) and standard deviation of the backscatter for one day (right) for October 23rd, 2020 over the Arctic area.

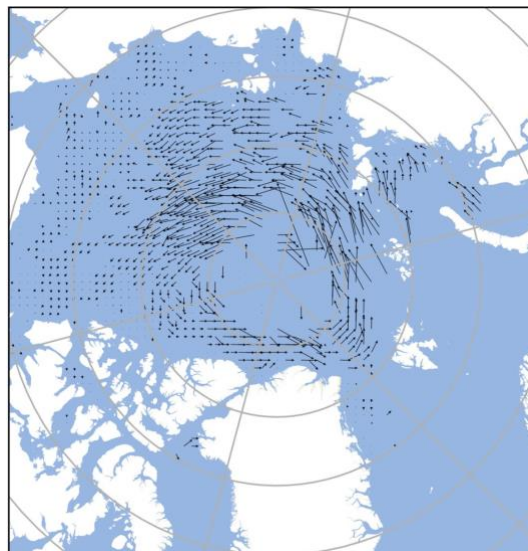


Figure 7: Sea ice drift January 1st to 4th, 2021 inferred from CFOSAT CSCAT data.

3.5 Sea ice type

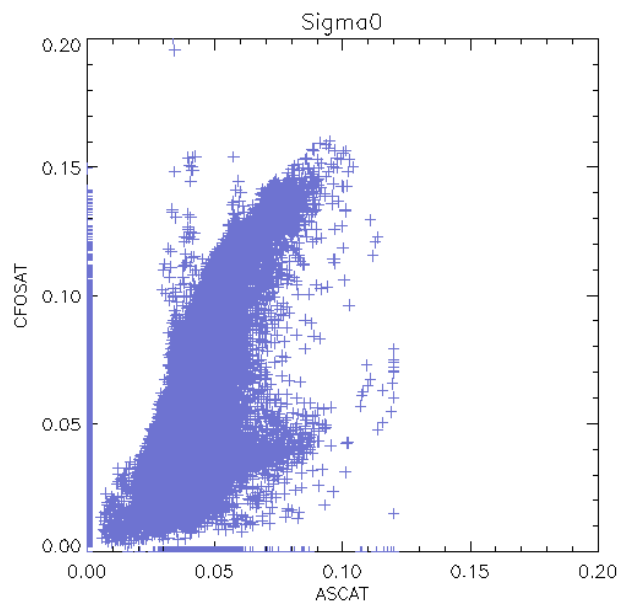


Figure 8: Sea ice backscatter plot CSCAT CFOSAT versus ASCAT. October 23rd, 2020. Unit is in linear dB.

Figure 8 shows the values of the backscatter over one day in winter for both ASCAT C-band and CSCAT CFOSAT Ku-band. The pattern of this plot is similar to C versus Ku-band backscatter plots done for QuikSCAT/ASCAT and for ERS/NSCAT (Ezraty and Cavanié 1997). It shows that values for ASCAT C-band are from 0 to 0.11 (linear dB unit) whereas they are from 0 up to 0.20 for CFOSAT Ku band data so that it is easier to separate first year sea ice (low values) from multiyear ice (high values) using Ku-band than C-band as expected thanks to the experience of QuikSCAT/ASCAT study.

We will apply a threshold to separate first year from multiyear, as it was done for ASCAT and QuikSCAT (Girard-Ardhuin and Ezraty, 2010) to estimate the relative part of first year and multiyear-ice over the winter, this is an ongoing work.

4. Conclusion and further plans

Ifremer provides a unique long-term time series of sea ice displacement delivered through CERSAT, and also available at the IAOS portal developed in INTAROS. We show in this report that CFOSAT data are of sufficient quality to be used to continue the time series. The calibration/validation activity of the CFOSAT data at Ifremer will continue until the end of the year to perform a full year season backscatter evaluation.

Our first results using CFOSAT show that the data can be used for sea ice characterization with the inferred sea ice parameters: ocean/ice limit, type, displacement (parameter added in INTAROS). The sea ice data will be available through the IWWOC center at Ifremer, the study is done jointly with CNES.

IFREMER had the opportunity to collaborate with University of Seattle during the project; this US team had a cruise in the Beaufort area in October-November 2019. IFREMER received support from ESA for this experiment through the INTAROS project so that SAR Sentinel Data could be acquired over the area of the experiment during few weeks. These data will be used on detecting SAR/ocean waves interaction at the sea ice edge from the joint use of Satellite data and buoys/boat data.

A tool has been applied to use joint data to detect sea ice phenomena in the MIZ (eddies), and a study has been started using the two sensors jointly (SWIM and CSCAT onboard CFOSAT) to see the benefit of the 2 sensors at the same time at the same place for polar studies.

5. Data exploitation

Because of the 2-year delay of the scatterometer CFOSAT reliable data, the cal/val activity is not yet finished at the end of INTAROS project but the work will continue end of 2021 and during 2022 and will be published after the end of the project.

The sea ice CFOSAT sea ice drift data will be added to the existing dataset using QuikSCAT and ASCAT to extent the Ifremer/CERSAT time series, and this new updated dataset will be available through the iAOS portal. Demonstrations and research activities around the use of the sea ice CFOSAT datasets will also refer to work done for the INTAROS project.

6. References

- Ezraty, R., A. Cavanié, 1999: Intercomparison of backscatter maps over Arctic sea ice from NSCAT and ERS scatterometers. *J. Geophys. Res.*, 114, C5, 11,471-483.
- Girard-Ardhuin, F., R. Ezraty, 2010: First year/multiyear ice detection using ASCAT and QuikSCAT data. EU DAMOCLES project report n. D1.2-01e.
- Girard-Ardhuin, F., R. Ezraty, 2012: Enhanced Arctic Sea ice drift estimation merging radiometer and scatterometer data. *IEEE Trans. Geosci. Remote Sensing*, vol. 50 (7), July 2012, pp 2639-2648. Doi : 10.1109/TGRS.2012.2184124.
- Le Traon, P.Y., Abadie, V., Ali, A., Aouf, L., Artioli, Y., Ascione, I., Autret, E., Aydogdu, A., Aznar, R., Baharel, P., Barrera, E., Bastide, L., Bazin, D., Behrens, A., Bentamy, A., Bertino, L., Böhm, E., Bonofiglio, L., Bourdallé Badie, R., Brando, V.E., Brandt-Kreiner, M., Bricaud, C., Bruciaferri, D., Buongiorno Nardelli, B., Buus-Hinkler, J., Cailleau, S., Calton, B., Carrasco, A., Carval, T., Cesarini, C., Chabot, G., Charles, E., Chau, T., Ciliberti, S., Cipollone, A., Claustre, H., Clementi, E., Colella, S., Colombo, F., Coppini, G., Cossarini, G., Crosnier, L., D'Alimonte, D., Dabrowski, T., De Alfonso, M., de Nuce, A., Delamarche, A., Derval, C., Di Cicco, A., Dibarboure, G., Dinessen, F., Dodet, G., Drevillon, M., Drillet, Y., Drudi, M., Durand, E., Escudier, R., Etienne, H., Fabardines, M., Faugère, Y., Fleming, A., Forneris, V., Garcia-Hermosa, I., Sotillo, M.G., Garnesson, P., Garric, G., Gasciarino, G., Gehlen, M., Giesen, R., Giordan, C., Girard-Ardhuin, F., Golbeck, I., Good, S., Gourrion, J., Gregoire, M., Greiner, E., Guinehut, S., Gutknecht, E., Harris, C., Hernandez, F., Hieronymi, M., Høyer, J., Huess, V., Husson, R., Jandt-Scheelke, S., Jansen, E., Kärnä, T., Karvonen J., Kay, S., King, R.R., Korres, G., Krasemann, H., Labrousse, C., Lagema, P., Lamouroux, J., Law Chune, S.,

Lecci, R., Legros, V., Lellouche, J.M., Levier, B., Li, X., Lien, V.S., Lima, L., Lindenthal, A., Linders, J., Lorente, P., Lorkowski, I., Mader, J., Maksymczuk, J., Maljutenko, I., Mangin, A., Marinova, V., Masina, S., Matreata, M., McConnell, N., Melet, A., Melsom, A., Messal, F., Morrow, R., Mouche, A., Mulet, S., Netting, J., Nord, A., Novellino, A., Obaton, D., Palazov, A., Pascual, A., Payet, J.M., Peneva, E., Pequignet, A.C., Perivolis, L., Perruche, C., Pfeil, B., Piollé, J.F., Pisano, A., Pistoia, J., Polton, J.A., Pouliquen, S., Pujol, M.I., Quade, G., Quéau, A., Ravdas, M., Reffray, G., Régnier, C., Renshaw, R., Reppucci, A., Rotlan, P., Ruggiero, G., Saldo, R., Salon, S., Samson, G., Santoleri, R., Saulter, A., Saux-Picart, E., Sauzède, R., Schwichtenberg, F., She, J., Siddorn, J., Skakala, J., Staneva, J., Stelzer, K., Stoffelen, A., Sykes, P., Szczypta, C., Szekely, T., Tamm, S., Tan, T.A., Tarot, S., Teruzzi, A., Thomas-Courcoux, C., Tintore, J., Titaud, O., Tonani, M., Tronci, M., Tuomi, L., Van der Zande, D., Vandenbulcke, L., Verbrugge, N., Volpe, G., von Schuckmann, K., Wakelin, S.L., Wedhe, H., Zacharioudaki, A., Zuo, H., 2021: The Copernicus Marine Service from 2015 to 2021: six years of achievements. *Special Issue Mercator Océan Journal* #57. DOI :<https://doi.org/10.48670/moi-cafr-n813>.

Sumata, H., T. Lavergne, F. Girard-Ardhuin, N. Kimura, M.A. Tschudi, F. Kauker, M. Karcher, R. Gerdes, 2014 : An intercomparison of Arctic ice drift products to deduce uncertainties estimates. *J. Geophys. Res. Ocean*, vol. 119, July 2014. DOI : 10.1002/2013JC009724.

Ifremer datasets access and user manuals are available at CERSAT portal: <http://cersat.ifremer.fr/>

The info-sheet data about the Ifremer/CERSAT sea ice drift datasets is available on the INTAROS project website.

----- END of DOCUMENT-----



INTAROS

This report is made under the project
Integrated Arctic Observation System (INTAROS)
funded by the European Commission Horizon 2020 program
Grant Agreement no. 727890.



Project partners:

